

## ELECTROMAGNETIC CASIMIR EFFECT IN WEDGE GEOMETRY AND THE ENERGY-MOMENTUM TENSOR IN MEDIA

I. BREVIK\* and S. Å. ELLINGSEN†

*Department of Energy and Process Engineering, Norwegian University of Science and  
Technology, N-7491 Trondheim, Norway*

*\*E-mail: iver.h.brevik@ntnu.no*

*†E-mail: simen.a.ellingsen@ntnu.no*

K. A. MILTON

*Oklahoma Center for High Energy Physics and H.L. Dodge Department of Physics  
and Astronomy, The University of Oklahoma, Norman, OK 73019, USA*

*E-mail: milton@nhn.ou.edu*

The wedge geometry closed by a circular-cylindrical arc is a nontrivial generalization of the cylinder, which may have various applications. If the radial boundaries are not perfect conductors, the angular eigenvalues are only implicitly determined. When the speed of light is the same on both sides of the wedge, the Casimir energy is finite, unlike the case of a perfect conductor, where there is a divergence associated with the corners where the radial planes meet the circular arc. We advance the study of this system by reporting results on the temperature dependence for the conducting situation. We also discuss the appropriate choice of the electromagnetic energy-momentum tensor.

### 1. Introduction

Casimir theory for the wedge geometry continues to attract interest. The reasons for this are many-faceted – probably the most important one being that the material boundaries are plane, thus avoiding some of the formal divergences that so often plague calculations in the presence of curved boundaries. The wedge geometry moreover implies a formalism closely related to that of cylindrical geometry, and actually also to that of cosmic string theory. Finally, the wedge geometry is a convenient testing ground for experimental tests of Casimir-Polder forces.

The Casimir energy and stress in a wedge geometry was approached already in the 1970s.<sup>1,2</sup> Various embodiments of the wedge with perfectly

conducting walls were treated by Brevik and co-workers<sup>3–5</sup> and others.<sup>6,7</sup> More recently a wedge intercut by a cylindrical shell was considered by Nesterenko and co-workers.<sup>8,9</sup> Local Casimir stresses were considered by Saharian and co-workers.<sup>10–12</sup> The interaction of an atom with a wedge was studied experimentally by Sukenik *et al.*<sup>13</sup> The theory of that interaction was worked out by Barton<sup>14</sup> and others.<sup>15–18</sup> The semitransparent wedge has very recently been considered by Milton, Wagner, and Kirsten.<sup>19</sup> The closely related case of circular symmetry has been treated in several papers, dealing with a perfectly conducting circular boundary,<sup>20–22</sup> as well as the case of a dielectric circular boundary.<sup>24–27</sup>

The typical wedge geometry is sketched in figure 1a. The planes are situated at  $\theta = 0$  and  $\theta = \alpha$ . We shall assume in the present paper that the interior of the wedge is filled with an isotropic medium of spatially constant and nondispersive refractive index  $n = \sqrt{\epsilon\mu}$ .

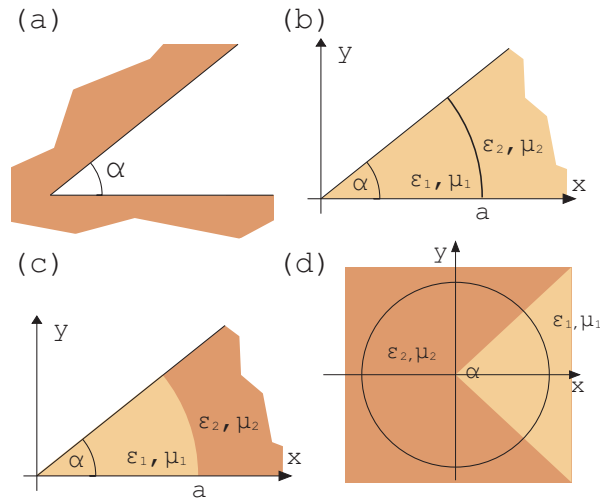


Fig. 1. Wedge geometries. (a) The perfectly conducting wedge geometry. (b) The geometry of a wedge intercut by a perfectly conducting cylindrical arc. (c) Wedge with magnetodielectric arc. (d) Diaphanous wedge in a perfectly conducting cylindrical shell.

In the simplest version of the wedge model, the planes are taken to be perfectly conducting. Various modifications of this simple wedge model can be envisaged. In sections 3 and 4 below we consider two generalizations of the simple wedge geometry, called Wedge I and II, in which the interior

region is closed by a circular boundary thus implying an eigenvalue problem for the photon frequencies. The Wedge II model treated in section 4, in particular, removes the strict perfect boundary condition of the radial walls. The material of these two sections is based on two recent papers.<sup>28,29</sup> New developments are a closer examination of the behavior at finite temperature. As an introductory step, we delineate in the next section the essentials of classic Casimir theory for the perfectly conducting wedge. In section 6 we relate the macroscopic electromagnetic theory for the dielectric wedge region to the more general question about which electromagnetic energy-momentum tensor is to be preferred in media. This one-hundred-year-old question has actually attracted considerable interest recently.

## 2. Extracts from the Classic Theory for the Perfectly Conducting Wedge

The geometry is shown in Fig. 1a and was considered in a number of publications.<sup>1-5</sup> The governing equation for the Fourier transform of Green's function  $\Gamma(x, x')$  is

$$\nabla \times \nabla \times \mathbf{\Gamma}(\mathbf{r}, \mathbf{r}', \omega) - \varepsilon\mu\omega^2\mathbf{\Gamma}(\mathbf{r}, \mathbf{r}', \omega) = -\mu\omega^2\mathbf{1}\delta(\mathbf{r} - \mathbf{r}'). \quad (1)$$

After solving this equation in terms of the scalar Green's functions  $F_m(r, r')$  and  $G_m(r, r')$ <sup>5</sup> we can calculate the effective field products for the electric fields as  $i\langle E_i(\mathbf{r})E_k(\mathbf{r}')\rangle_\omega = \Gamma_{ik}(\mathbf{r}, \mathbf{r}', \omega)$ . The corresponding products for the magnetic fields follow from Maxwell's equations. The points  $\mathbf{r}$  and  $\mathbf{r}'$  are assumed to be close but not coincident.

The effective products can now be inserted in the electromagnetic energy-momentum tensor  $S_{\mu\nu}$ , whose spatial part in classical notation is, in Heaviside-Lorentz units,

$$S_{ik} = -E_i D_k - H_i B_k + \frac{1}{2}\delta_{ik}(\mathbf{E} \cdot \mathbf{D} + \mathbf{H} \cdot \mathbf{B}). \quad (2)$$

A lengthy calculation leads to the expression (Minkowski metric assumed)

$$\langle S_{\mu\nu}(\mathbf{r}) \rangle = \frac{1}{720\pi^2\eta} \frac{1}{r^4} \left( \frac{\pi^2}{\alpha^2} + 11 \right) \left( \frac{\pi^2}{\alpha^2} - 1 \right) \text{diag}(1, -3, 1, 1), \quad (3)$$

where we have subtracted off the term  $\langle S_{\mu\nu}^{\alpha=\pi}(\mathbf{r}) \rangle$  corresponding to a plane sheet. The components are ordered as  $\langle S_{\mu\nu} \rangle = \langle S_{rr}, S_{\theta\theta}, S_{zz}, -w \rangle$ , where  $w$  is the energy density.

The expression (3) refers to zero temperature. It is worth noticing that in the limit  $\alpha \rightarrow 0, r \rightarrow \infty$  such that  $\alpha r$  becomes the separation between

parallel plates, the expression agrees with Barton.<sup>14</sup> Moreover, the expression agrees with that of a cosmic string if the string's deficit angle  $8\pi GM$  is identified with  $2\pi - 2\alpha$ .<sup>28</sup>

### 3. Wedge I: Perfectly Conducting Walls; Circular Boundary at $r = a$

The geometry is shown in Fig. 1b and 1c. The walls are perfectly conducting as before, while we assume now that there is as boundary a circular arc with radius  $a$ . The wedge thus has an interior region  $r < a$  (region 1) where the material parameters are  $\varepsilon_1$  and  $\mu_1$ , and an exterior region  $r > a$  (region 2) with analogous parameters  $\varepsilon_2$  and  $\mu_2$ . The materials are assumed to be nondispersive. We assume the diaphanous (isorefractive) condition  $\varepsilon_1\mu_1 = \varepsilon_2\mu_2 = n^2$ . The transverse wave numbers  $k_\perp$  in the two regions are accordingly the same,  $k_\perp^2 = n^2\omega^2 - k_z^2$ . It is convenient to introduce the symbol  $p = \pi/\alpha$ , and also  $\lambda_\nu(x) = (I_\nu(x)K_\nu(x))'$ , where  $I_\nu$  and  $K_\nu$  are modified Bessel functions.

#### 3.1. The boundary $r = a$ being perfectly conducting

This is the simplest case. Detailed expansions of the electric and magnetic fields are given in Ref. 28. In region 1 there are two independent polarizations, one TM polarization where the mode eigenvalues are determined by  $J_{mp}(k_\perp a) = 0$  with  $m = 1, 2, 3, \dots$ , and one TE polarization where the eigenvalues are determined by  $J'_{mp}(k_\perp a) = 0$ . One azimuthally symmetric TE mode exists, corresponding to  $m = 0$ , but there is no such TM mode.

In region 2 the TM polarization yields  $H_{mp}^{(1)}(k_\perp a) = 0$ ,  $m = 1, 2, 3, \dots$ , whereas the TE polarization yields  $H_{mp}^{(1)'}(k_\perp a) = 0$ ,  $m = 0, 1, 2, \dots$ . Summing over all modes and making use of the argument principle, we arrive at the following expression for the total zero-point energy

$$\tilde{\mathcal{E}} = \frac{1}{4\pi na^2} \sum'_{m=0} \int_0^\infty dx x \ln[1 - x^2 \lambda_{mp}^2], \quad (4)$$

the prime meaning that the mode  $m = 0$  is counted with half weight. This is the boundary-induced contribution to the zero-point energy. If the boundary  $r = a$  were removed and either the interior or the exterior medium were to fill the whole region, we would get  $\tilde{\mathcal{E}} = 0$ . Moreover, we have omitted a zero-mode divergence caused by the sharp corners where the arc meets the wedge. If  $p = 1$ , Eq. (4) is one-half that for a conducting circular cylinder.

### 3.2. Dielectric boundary at $r = a$

The most important change compared with the previous subsection is that regions 1 and 2 become coupled via electromagnetic boundary conditions. Assuming  $n_1 = n_2$  we find the following simple expression for the zero-point energy

$$\tilde{\mathcal{E}} = \frac{1}{4\pi na^2} \sum_{m=0}^{\infty} ' \int_0^{\infty} dx x \ln[1 - \xi^2 x^2 \lambda_{mp}^2], \quad (5)$$

with

$$\xi = \frac{\varepsilon_2 - \varepsilon_1}{\varepsilon_2 + \varepsilon_1}. \quad (6)$$

The conducting case is obtained by setting  $\xi = 1$ . The case  $n_1 \neq n_2$  is more complicated, but for weak-coupling,  $|\varepsilon_1 - \varepsilon_2| \ll 1$ , a self-energy can still be extracted<sup>28</sup> by generalizing the work done on dielectric cylinders.<sup>24,25</sup>

The expressions (4) and (5) are still not in general finite. A finite self-energy can be extracted from this formula by a method of zeta function regularisation,<sup>23</sup> generalizing the standard formal result for a circular cylinder ( $p = 1$ ).<sup>20</sup> Further details and numerical results are reported in Ref. 28.

## 4. Wedge II: Diaphanous (Isorefractive) Wedge in cylindrical shell.

Consider the geometry of Fig. 1d wherein a diaphanous magnetodielectric wedge ( $n_1 = n_2$ ) inside a perfectly conducting cylindrical shell of radius  $a$  is considered. More details were published in Ref. 29. The sum over orders of the Bessel function partial waves is now not simply equidistant values  $\nu = mp$  as before but the zeros of the dispersion function for  $\nu = i\eta$ :

$$D(i\eta; \alpha) = \sinh^2 \eta\pi - \xi^2 \sinh^2 \eta(\pi - \alpha). \quad (7)$$

The reflection coefficient  $\xi$  was defined in Eq. (6). In the absence of any wedge this becomes  $D_0(i\eta) = \sinh^2 \eta\pi$ . The energy of the diaphanous wedge enclosed by a perfectly conducting cylindrical shell is thus found as

$$\tilde{\mathcal{E}} = \frac{1}{16\pi^3 i} \int_{-\infty}^{\infty} dk \int_{-\infty}^{\infty} d\zeta \zeta \int_{-\infty}^{\infty} d\eta \left( \frac{D'}{D} - \frac{D'_0}{D_0} \right) \frac{d}{d\zeta} \ln[1 - x^2 \lambda_{i\eta}^2(x)]. \quad (8)$$

In the non-dispersive case where  $\xi$  is independent of  $\zeta$  this may be simplified by means of partial integration w.r.t.  $\zeta$ , introduction of polar coordinates, and use of symmetry properties, to

$$\tilde{\mathcal{E}} = -\frac{1}{4\pi^2 na^2} \int_0^{\infty} d\eta \left( \frac{D'}{D} - \frac{D'_0}{D_0} \right) \int_0^{\infty} dx x \operatorname{Im} \ln[1 - x^2 \lambda_{i\eta}^2(x)]. \quad (9)$$

Since  $\text{Re}\{x^2\lambda_{i\eta}^2\} \leq 1$  we may use for numerical purposes

$$\text{Im} \ln(1 - x^2\lambda_{i\eta}^2) = -\arctan \frac{x^2 \text{Im}\lambda_{i\eta}^2}{1 - x^2 \text{Re}\lambda_{i\eta}^2}.$$

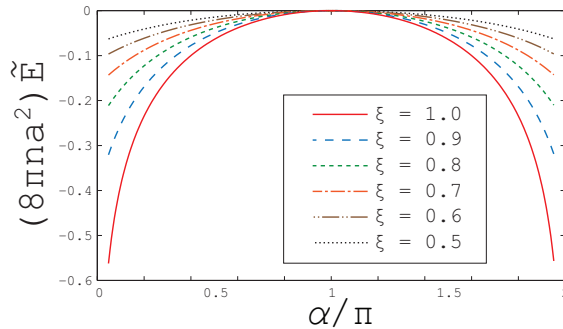


Fig. 2. The energy per length of the wedge, divided by a reference energy  $(8\pi na^2)^{-1}$ , as a function of opening angle  $\alpha$  for different values of the reflection coefficient  $\xi$ .

A numerical evaluation of this energy expression was performed in Ref. 29 and the details of the procedure will not be iterated here. The energy is plotted as a function of the opening angle  $\alpha$  for different values of the reflection coefficient  $|\xi|$  in Fig. 2.

## 5. Considerations of finite temperature

We present for the first time some considerations on the Casimir energy of a closed perfectly conducting wedge such as in figure 1b when  $T > 0$ . (For earlier work on the cylinder at high temperatures see Ref. 30.) By letting  $p = 1$  in the following, these considerations automatically apply to the case of the perfectly conducting cylinder. We consider the finite part of the energy, given for zero  $T$  in equation (4). As is customary, finite temperature implies a compactification of the imaginary time axis so that the integral over imaginary frequencies  $i\zeta$  becomes a sum over Matsubara frequencies  $\zeta_j = 2\pi jT$ :

$$\int_0^\infty d\zeta f(\zeta) \rightarrow 2\pi T \sum_{j=0}^{\infty} f(\zeta_j). \quad (10)$$

A little calculation shows that the expression (4) may then be written  $\tilde{\mathcal{E}} = \sum_{m=0}^{\infty'} \mathcal{E}_m$  where

$$\mathcal{E}_m = \frac{T}{\pi a} \sum_{j=0}^{\infty'} \int_{j\tau}^{\infty} \frac{dx x}{\sqrt{x^2 - j^2\tau^2}} \ln[1 - x^2 \lambda_{mp}^2(x)] = \frac{T}{\pi a} \sum_{j=0}^{\infty'} e_{m,j}. \quad (11)$$

The nondimensional temperature is  $\tau = 2\pi naT$ . As previously encountered at zero temperature the simple expression for  $\tilde{\mathcal{E}}$  is divergent and the challenge is to regularize it. We follow a scheme closely analogous to that of Ref. 23 (c.f. appendix A of Ref. 28) using zeta functions by subtracting and adding the asymptotic behaviour of the integrand,

$$\ln[1 - x^2 \lambda_{mp}^2(x)] \sim -\frac{x^4}{4(m^2 p^2 + x^2)^3}, \quad m, x \rightarrow \infty. \quad (12)$$

This asymptotic behaviour is responsible for divergences both for  $j \rightarrow \infty$  and  $m \rightarrow \infty$ . The work on this problem is still in progress and details of the calculations and further discussion will be published elsewhere.<sup>31</sup>

Adding and subtracting the asymptotic behaviour we write

$$\mathcal{E}_m = \frac{T}{\pi a} \sum_{j=0}^{\infty'} \left[ \tilde{e}_{\underline{m},j} - \frac{1}{4} \int_{j\tau}^{\infty} \frac{dx x^5}{\sqrt{x^2 - j^2\tau^2} (\underline{m}^2 p^2 + x^2)^3} \right], \quad (13)$$

using compact notation  $\underline{m}$  defined as  $\underline{m}(m) = m$  for  $m \geq 1$  and  $\underline{m}(0) = 1/p$ . The symbol  $\tilde{e}$  implies that the leading asymptotic term (12) has been subtracted from the integrand, with  $\underline{m}$  replacing  $m$ . The double sum resulting from the integral in (13) is formally divergent but may be regularised by use of the Chowla-Selberg formula.<sup>32</sup> After some calculation we obtain the following result

$$\tilde{\mathcal{E}} = \frac{T}{\pi a} \sum_{m,j=0}^{\infty'} \tilde{e}_{\underline{m},j} - \frac{\tau(3 - 3\tau\partial_\tau + \tau^2\partial_\tau^2)[1 + 2\mathcal{K}(\tau) + \mathcal{S}(\tau, p)]}{512\pi na^2}; \quad (14a)$$

$$\mathcal{K}(\tau) = \sum_{j=1}^{\infty} \frac{j\tau - \sqrt{1 + j^2\tau^2}}{j\tau\sqrt{1 + j^2\tau^2}}, \quad (14b)$$

$$\mathcal{S}(\tau, p) = \frac{2}{p}[\gamma - \ln(4\pi p/\tau)] + \frac{8}{p} \sum_{l=1}^{\infty} \sigma_0(l) K_0(2\pi l\tau/p), \quad (14c)$$

where  $\gamma$  is Euler's constant,  $\sigma_0(l)$  is the number of positive divisors of  $l$ ,  $K_0$  is the modified Bessel function of the second kind, and  $\partial_\tau = \partial/\partial\tau$ . Notably,  $\mathcal{S}$  obeys the symmetry relation  $\mathcal{S}(\tau, p) = \mathcal{S}(p, \tau)$ . One may show that this result reduces to the zero temperature expression<sup>28</sup> when  $\tau \rightarrow 0$ ,<sup>31</sup> and we have verified that when  $p = 1$  the coefficients of the two leading-order terms

as  $\tau \rightarrow \infty$ , of order  $\tau$  and  $\tau \ln \tau$ , equal twice those found previously for the cylindrical shell in Ref. 30 as they should.

## 6. On the Electromagnetic Energy Momentum Tensor in Media

The expression (2) for the spatial part of the energy-momentum tensor (equal to minus the Maxwell stress tensor  $T_{ik}$  according to Møller<sup>33</sup>), is common for the Minkowski and Abraham tensor alternatives as long as the medium is isotropic. The extraction of the “correct” form of the tensor has however been discussed for a long time. Thus it is to be noted that

- the expression is different from that of Einstein and Laub (1908);<sup>34</sup>
- it is different from that of Peierls (1976);<sup>35</sup>
- and it is different from that of Raabe and Welsch (2005);<sup>36</sup> cf. also the comment<sup>37</sup> of Brevik and Ellingsen. A survey up to 1979 is given by Brevik.<sup>38</sup>

When combined with the Minkowski momentum density  $\mathbf{g}^M = \mathbf{D} \times \mathbf{B}$  one obtains the Minkowski energy-momentum tensor  $S_{\mu\nu}^M$  whose covariant form can be written as<sup>33</sup>

$$S_{\mu\nu}^M = F_{\mu\alpha}H_{\nu\alpha} - \frac{1}{4}\delta_{\mu\nu}F_{\alpha\beta}H_{\alpha\beta}. \quad (15)$$

Here  $F_{4k} = iE_k$ ,  $H_{4k} = iD_k$ ,  $F_{ik} = B_l$  (cycl),  $H_{ik} = H_l$  (cycl). This energy-momentum tensor has several attractive properties: it has zero divergence for a pure radiation field, the four components of momentum and energy forming a four-vector; it is a convenient expression for field quantization (for instance, the quantization for a radiation field in a nondispersive medium can be found via a mapping technique leading one from vacuum to a medium<sup>39</sup>), and it has the peculiar property of being a space-like expression leading to negative photon energies in certain coordinate systems, strikingly found in connection with the Cherenkov effect in the emitter’s rest frame.

One might think that it should be relatively easy to test the Minkowski tensor by measuring electromagnetic forces in optics. Actually, this is not so easy as most experiments measure only the surface force density  $\mathbf{f} = -\frac{1}{2}E^2\nabla\epsilon$ , acting on surfaces. Let us give some examples:

The classic experiment of Ashkin and Dziedzic<sup>40</sup> showed how a narrow light beam incident on a free liquid surface acts by giving rise to an outward pull. A related experiment is that of Zhang and Chang,<sup>41</sup> demonstrating the oscillations of a water droplet by a laser pulse. The optical stretcher



experiment of Guck *et al.*<sup>42</sup> is of the same kind, as is the series of two-fluid experiments of Delville *et al.*<sup>43</sup> near the critical point. The important factor in these experiments is simply the surface force, not electromagnetic momentum. And the recent fiber experiment of She *et al.*<sup>44</sup> belongs in our opinion to the same category.<sup>45</sup> The experiment of Campbell *et al.*<sup>46</sup> is however different in nature, as it is one of the very few experiments being able to test the Minkowski momentum directly.

Under stationary conditions, where the high-frequency forces average out when averaged over a period, the Minkowski tensor is able to describe all experiments that we are aware of. And this gives support to our expression (2) for the stress tensor.

The work of KAM was supported by the US National Science Foundation under Grant No. PHY-0554926 and by the US Department of Energy under Grants Nos. DE-FG02-04ER41305 and DE-FG02-04ER-46140.

## References

1. J.S. Dowker and G. Kennedy, *J. Phys. A* **11**, 895 (1978).
2. D. Deutsch and P. Candelas, *Phys. Rev. D* **20**, 3063 (1979).
3. I. Brevik and M. Lygren, *Ann. Phys.* **251**, 157 (1996).
4. I. Brevik, M. Lygren, and V. Marachevsky, *Ann. Phys.* **267**, 134 (1998).
5. I. Brevik and K. Pettersen, *Ann. Phys.* **291**, 267 (2001).
6. V.V. Nesterenko et al., *Ann. Phys.* **298**, 403 (2002).
7. H. Razmi and S.M. Modarresti, *Int. J. Mod. Phys.* **44**, 229 (2005).
8. V.V. Nesterenko et al., *J. Math. Phys.* **42**, 1974 (2001).
9. V.V. Nesterenko et al., *Class. Quant. Grav.* **20**, 431 (2003).
10. A.H. Rezaeian and A.A. Saharian, *Class. Quant. Grav.* **19**, 3625 (2002).
11. A.A. Saharian, *Eur. Phys. J. C* **52**, 721 (2007).
12. A.A. Saharian, Casimir densities for wedge-shaped boundaries, in *The Casimir Effect and Cosmology*, (Tomsk State Pedagogical University Press, Tomsk, Russia, 2008), [arXiv: 0810.5207](https://arxiv.org/abs/0810.5207).
13. C.I. Sukenik et al., *Phys. Rev. Lett.* **70**, 560 (1993).
14. G. Barton, *Proc. R. Soc. London* **410**, 175 (1987).
15. S.C. Skipsey et al., *Opt. Commun.* **254**, 262 (2005).
16. S.C. Skipsey et al., *Phys. Rev. A* **73**, 011803(R) (2006).
17. T.N.C. Mendes et al., *J. Phys. A* **41**, 164029 (2008).
18. F.S.S. Rosa et al., *Phys. Rev. A* **78**, 012105 (2008).
19. K.A. Milton, J. Wagner, and K. Kirsten, [arXiv:0911.1123](https://arxiv.org/abs/0911.1123), *Phys. Rev. D*, in press.
20. L.L. DeRaad, Jr and K.A. Milton, *Ann. Phys.* **136**, 229 (1981).
21. P. Godzinsky and A. Romeo, *Phys. Lett. B* **441**, 265 (1998).
22. G. Lambiase et al., *J. Math. Phys.* **40**, 6254 (1999).
23. K.A. Milton et al., *Phys. Rev. D* **59**, 105009 (1999).
24. I. Cavero-Peláez and K.A. Milton, *Ann. Phys.* **320**, 108 (2005).

25. I. Cavero-Peláez and K.A. Milton, *J. Phys. A* **39**, 6225 (2006).
26. A. Romeo and K. A. Milton, *Phys. Lett. B* **621**, 309 (2005).
27. I. Brevik and A. Romeo, *Phys. Scripta* **76**, 48 (2007).
28. I. Brevik, S.Å. Ellingsen, and K.A. Milton, *Phys. Rev. E* **79**, 041120 (2009).
29. S.Å. Ellingsen, I. Brevik, and K.A. Milton, *Phys. Rev. E* **80**, 021125 (2009).
30. M. Bordag, V.V. Nesterenko, and I.G. Pirozhenko, *Phys. Rev. D* **65**, 045011 (2002); *Nucl. Phys. B* **104**, 228 (2002).
31. S.Å. Ellingsen, I. Brevik, and K.A. Milton, in preparation.
32. E. Elizalde, *Ten Physical Applications of Spectral Zeta Functions* (Springer, Berlin, 1995), p.83.
33. C. Møller, *The Theory of Relativity* (Clarendon Press, Oxford, 1972).
34. A. Einstein and J. Laub, *Ann. Physik* **26**, 541 (1908).
35. R. Peierls, *Proc. Roy. Soc. A* **347**, 475 (1976).
36. C. Raabe and D.-G. Welsch, *Phys. Rev. A* **71**, 013814 (2005).
37. I. Brevik and S. A. Ellingsen, *Phys. Rev. A* **79**, 027801 (2009); cf. also Reply *ibid.* (in press).
38. I. Brevik, *Phys. Rep.* **52**, 133 (1979).
39. I. Brevik and B. Lautrup, *Mat. Fys. Medd. Dan. Vid. Selsk.* **38**, No. 1 (1970).
40. A. Ashkin and J.M. Dziedzic, *Phys. Rev. Lett.* **30**, 139 (1979).
41. J.Z. Zhang and R.K. Chang, *Opt. Lett.* **13**, 916 (1988).
42. J. Guck *et al.*, *Biophys. J.* **81**, 767 (2001).
43. J.P. Delville *et al.*, *Trends in Electro-Optic Research* (Nova Sciences, New York, 2006), pp. 1-58.
44. W. She *et al.*, *Phys. Rev. Lett.* **101**, 243601 (2008).
45. I. Brevik, *Phys. Rev. Lett.* **103**, 219301 (2009); cf. also Reply *ibid.* **103**, 219302 (2009).
46. G.K. Campbell *et al.*, *Phys. Rev. Lett.* **94**, 170403 (2005).
47. R.V. Jones and J.C.S. Richards, *Proc. Roy. Soc. London Ser. A* **221**, 480 (1954).